Iterative Analysis Method for Structural Components with Diverse Stiffnesses

I.U. Ojalvo,* F. Austin,† and A. Levy‡
Grumman Aerospace Corporation, Bethpage, N.Y.

An iterative solution scheme is presented for the static and dynamic analysis of built-up structures in which the stiffness of one relatively rigid component is a dominant factor in governing the overall response. In complex problems, where each structural component is represented by finite-element models with many degrees of freedom, application of the standard direct-stiffness method requires equation solutions involving large numbers of unknowns. Also, the direct stiffness method may lead to numerical precision problems when combining the terms of components with diverse stiffnesses. This paper presents a technique which, under certain conditions to be discussed, overcomes these problems through an efficient iterative procedure. The method requires treatment of only a single structural component at any given time and the convergence rate is shown to depend upon the relative impedances of the components. Results are presented for the static, dynamic, and thermal stress analysis of the space-shuttle thermal-protection system. This problem is ideally suited to this application and results reveal a rapid rate of convergence.

Introduction

THIS paper presents an iterative procedure for the static and dynamic analysis of built-up structures. The method is based on a technique proposed by Newman and Goldberg[1] for the static analysis of an ablative heat shield. This procedure was designed to determine stresses induced by thermal gradients and mechanical loads, in a geometrically complex ablator material. In this work, the method is extended to include free-vibration problems as well. Conditions for convergence of the procedure are discussed. These conditions are exact for statics problems but only approximate for free vibrations if the frequency is not known a priori.

The general configuration considered herein is shown in Fig. 1a. It consists of a relatively stiff primary-structure to which one or more components, comprising a relatively flexible secondary-structure, are attached. An example of this configuration, for which numerical results are presented, is the thermal protection system (TPS) of the reusable space shuttle orbiter. The TPS consists of numerous reusable surface insulation (RSI) tiles bonded to the metal skin of the orbiter through a soft strain isolation layer. The stiffened skin of the orbiter comprises the primary-structure which, in general, dominates the deformation of the system. The tiles are taken as the secondary (much less stiff) components. The details of this application are contained in Refs. 2-4.

General Description of the Method

The basis for the method is that the secondary-structure is nonstructural but its stress levels, which are often critical for integrity of the system, must be computed. Thus, it becomes possible to neglect the stiffness of the secondary-structure initially, but not its mass, to determine approximate primary-structure deflections.

The basic method, as applied to statics and thermal stress problems, is illustrated in Fig. 1. In the initial calculations, the statical equivalence of the external mechanical loads P acting on the secondary-structure are applied directly to the primary-structure, and its deflections δ_B are obtained (see Fig. 1b). An iteration procedure is then performed where, in each step, the resulting primary-structure deflections are imposed individually on each component of the secondary-structure (see Fig. 1c) at the secondary/primary-structure interface, and the remaining secondary-deflections and interface boundary loads V_B and H_B are computed. The secondary-structure interface loads obtained are then assembled and their reaction $-V_B$ and $-H_B$ are applied to the primary structure as shown in Fig. 1d. New primary-structure deflections δ'_B are obtained and compared to the previous set. This procedure is repeated until convergence of results is achieved. The logic is outlined in Fig. 2.

The logic for the calculation of the vibration modal characteristics is outlined in Fig. 3. In the initial calculations, the stiffness, but not the mass, of the secondary-structure is neglected in order to obtain approximations to the natural frequencies and mode shapes. An iterative procedure is then performed where the primary-structure oscillatory modal deflections are imposed individually on each component of the secondary-structure at the secondary/primary-structure interface, and the steady-state component deflections and interface boundary loads are obtained. The frequency is then updated by computing a Rayleigh quotient, using the latest nonrigid component displacements. The individual secondary component boundary loads obtained are then assembled and their reactions applied to the primary-structure. New primary-structure deflections are obtained, normalized, and then compared to the previous set. This process is repeated for a given mode until convergence of frequency and mode shape is obtained.

By these methods, each component of the secondary-structure is temporarily assumed uncoupled from all others. Although this is not strictly true, under proper conditions (to be discussed) the coupling involved is sufficiently weak so as to ensure accurate, approximate results in early iterations as well as rapid convergence. This treatment of each component as an uncoupled problem often results in a significant savings in computer running times and storage requirements. In fact, certain problems (such as the space-shuttle TPS) that appeared too large to treat in great detail by the direct stiffness method, have been found to be quite tractable by this technique.

Analysis of Typical Secondary-Structure Component

The secondary-structure components are originally treated as nonstructural mass items. However, since their stress states

Presented as Paper 75-801 (Ref. 4) at the AIAA/ASME/SAE 16th Structures, Structural Dynamics, and Materials Conference, Denver, Colo., May 27-29, 1975; submitted September 2, 1975; revision received February 26, 1976. This work was sponsored by the NASA Langley Research Center under Contracts NAS 1-10635-17 and -19. The authors are grateful to P. Ogilive for here invaluable assistance in the development of the computer program associated with this effort.

Index categories: Structural Static Analysis; Structural Dynamic Analysis; Thermal Stresses.

*Structural Methods Engineer.
†Group Specialist, Structural Mechanics Section.
‡Research Scientist. Member AIAA.

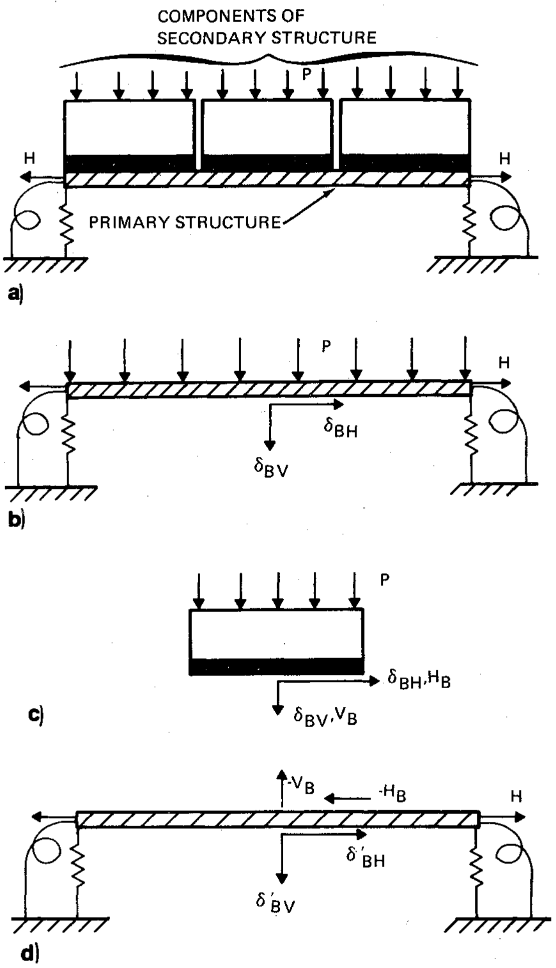

Fig. 1 Iterative approach for statics and thermal stress problems: a) Complete problem. b) Initial primary structure problem with first approximation to primary structure deflections. c) Typical problem for each component of secondary structure; interface deflections are imposed and boundary reactions computed. d) Recomputation of primary structure deflections; compare deflection with previous iteration.

are desired, it is necessary to eventually account for their stiffnesses. This is achieved by imposing the primary/secondary-structure component interface deflections, $(\delta_B)_i \cos\omega t$, on each component and computing its associated internal deflections, $(\delta_A)_i \cos\omega t$, and corresponding stresses and reactions, $(-P_B)_i \cos\omega t$. As described earlier, this is done iteratively until convergence is obtained.

Referring to Fig. 4, the associated steady-state partitioned matrix equations governing each secondary-component are

$$\begin{bmatrix} K_{AA}-\omega^2 M_{AA} & K_{AB} \\ K_{BA} & K_{BB}-\omega^2 M_{BB} \end{bmatrix} \begin{Bmatrix} \delta_A \\ \delta_B \end{Bmatrix}_i = \begin{Bmatrix} P_A+\bar{P}_A \\ P_B+\bar{P}_B \end{Bmatrix}_i \tag{1}$$

where the subscript B is used to denote points of the secondary components which are in common to the primary structure. Use has been made of the fact that the component mass matrix is diagonal, the $\bar{P}$' s refer to thermal loading terms, and P_A is a statically applied external loading. For free-vibration problems, all the P' s with the exception of P_B, are taken as zero in Eq. (1). For static problems, ω is taken as zero.

$$[K_{AA}-\omega^2 M_{AA}]\ \{\delta_A\}_i = -[K_{AB}]\ \{\delta_B\}_i + \{P_A+\bar{P}_A\}_i \tag{2}$$

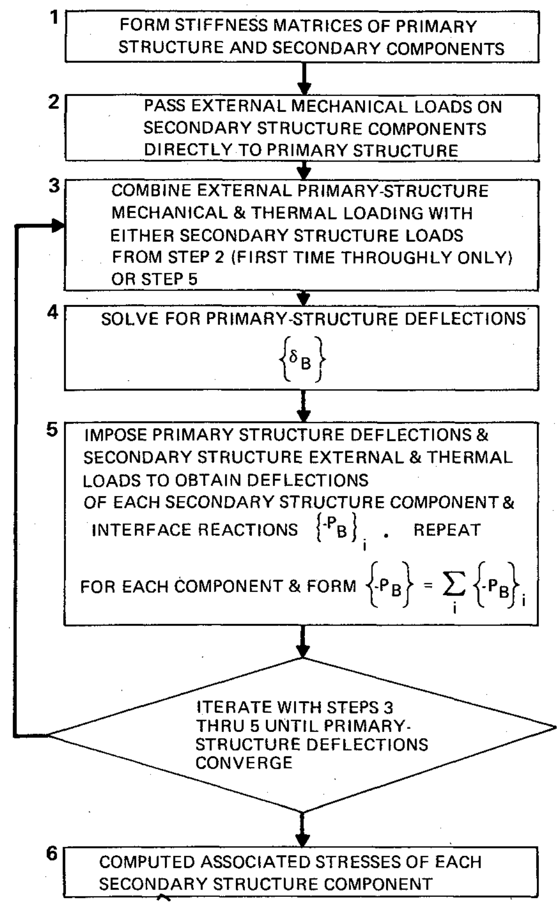

Fig. 2 Logic for statics and thermal stress problems.

and

$$\{\bar{P}_B\}_i - [K_{BA}]\ \{\delta_A\}_i - [K_{BB}-\omega^2 M_{BB}]\ \{\delta_B\}_i = \{-P_B\}_i \tag{3}$$

Equation (2) is next solved for $\{\delta_A\}_i$, which is then substituted into Eq. (3) for $\{-P_B\}_i$. Once convergence of δ_B has been achieved, the secondary-structure stresses are computed from the associated stress recovery equations.

Frequency Update

Since the modes and frequencies obtained originally ignored the secondary-structure stiffness and true displacements, the resulting frequencies are only approximate. To correct these, the frequencies are updated through use of a Rayleigh-quotient calculation in which the latest secondary- and primary-structure deflections are used in the equation

$$\omega_R^2 = \frac{\Sigma_i \lfloor \delta_S \rfloor_i [K_S] \{\delta_S\}_i + \lfloor \delta_{ps} \rfloor [K_{ps}] \{\delta_{ps}\}}{\Sigma_i \lfloor \delta_S \rfloor_i [M_S] \{\delta_S\}_i + \lfloor \delta_{ps} \rfloor [M_{ps}] \{\delta_{ps}\}} \tag{4}$$

where the subscripts S and ps denote secondary and primary structure, respectively. Thus, $\{\delta_{ps}\}$ are the latest primary-structure deflections, and $[K_{ps}]$ and $[M_{ps}]$ are the banded stiffness and mass matrices, respectively, of the primary structure. The secondary-component stiffness and mass matrices, $[K_S]$ and $[M_S]$, respectively, of Eq. (4) are related to the stiffness and mass matrices of Eq. (2):

$$[K_S] = \begin{bmatrix} K_{AA} & K_{AB} \\ K_{BA} & K_{BB} \end{bmatrix} \qquad [M_S] = \begin{bmatrix} M_{AA} & 0 \\ 0 & M_{BB} \end{bmatrix}$$

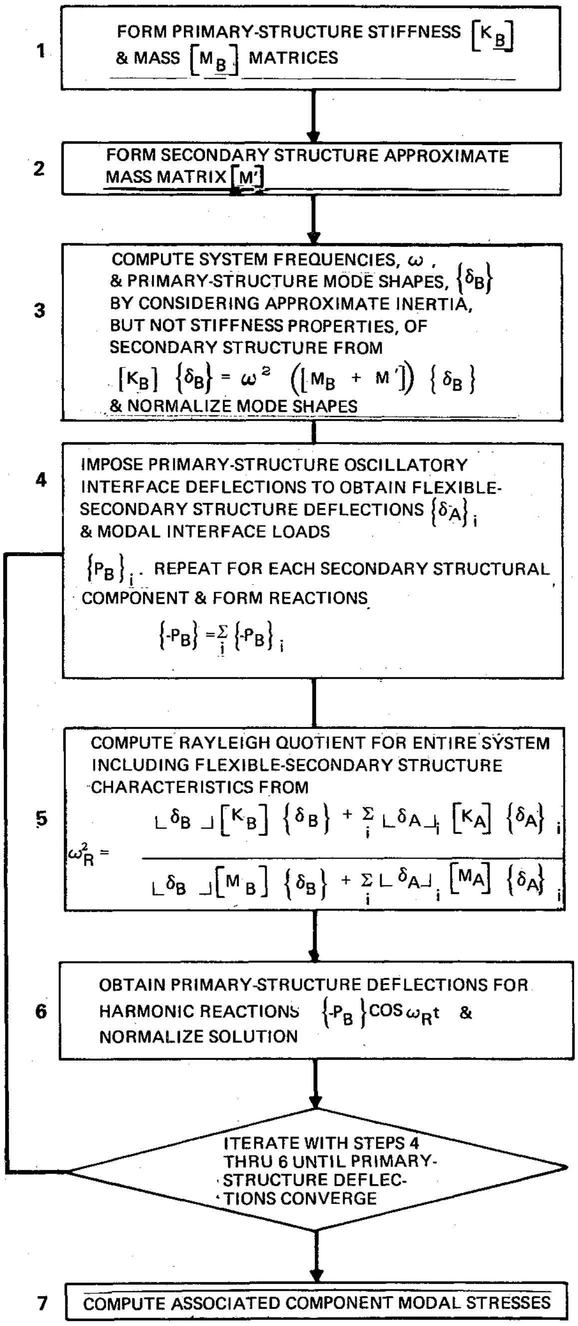

Fig. 3 Program logic for natural-vibration problems.

Primary-Structure Deflection Update

The original primary-structure deflections are approximate. They should be checked and, if necessary, corrected. For vibration problems, the frequencies are recomputed, employing the latest compatible set of secondary- and primary-structure deflections, to give ω_{Rayleigh} by the method described in the previous subsection. The boundary reactions $\{-P_B\}_i \cos\omega_R t$ are collected for all components of the secondary structure and applied to the primary structure to yield new deflections:

$$[K_{ps}-\omega_R^2 M_{ps}]\ \{\delta_{ps}\}=\{-P_B\}+\{P_{ps}\}+\{\bar{P}_{ps}\} \tag{5}$$

where $\{-P_B\}\cos\omega_R t$ is the assembled load reaction of all the secondary-structure components acting on the primary structure.

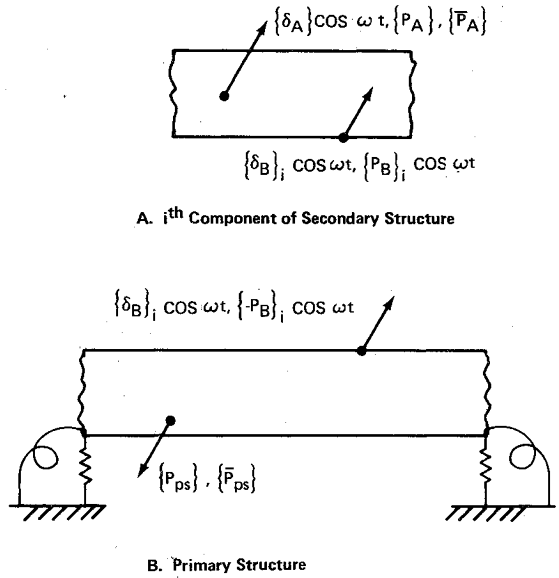

Fig. 4 Notation for analysis of *i*th component of secondary structure. Note: Barred terms, $\bar{P}_A$ and $\bar{P}_{ps}$ refer to "thermal loads."

The convergence test consists in satisfying

$$\max\left\{\left|\delta_{ps_{\text{present}}}-\delta_{ps_{\text{previous}}}\right|\right\}\le\epsilon\left\{\max\left|\delta_{ps_{\text{present}}}\right|\right\}$$

where ϵ is an arbitrarily small positive quantity.

Convergence Condition

As shown in Ref. 5, the mathematical condition for absolute convergence of the present iteration procedure is that the maximum absolute eigenvalue, $\lambda_{\max}$, of the equation

$$[K_s']\ \{\delta_{ps}\}=\lambda[K_{ps}]\ \{\delta_{ps}\} \tag{6}$$

must satisfy the condition

$$\lambda_{\max}<1 \tag{7}$$

A similar derivation based upon impedances Z leads to the condition

$$|\lambda|_{\max}<1 \tag{8}$$

where

$$[Z_s']\ \{\delta_{ps}\}=\lambda[Z_{ps}]\ \{\delta_{ps}\} \tag{9}$$

when ω_R^2 is a good estimate of ω^2, and where the impedances, Z, are related to the previously defined stiffnesses and masses:

$$[Z_s']\equiv[\bar{Z}_{BB}]-[\bar{K}_{BA}]\ [\bar{Z}_{AA}]^{-1}[\bar{K}_{AB}]$$
$$[Z_{ps}]=[K_{ps}-\omega^2 M_{ps}]$$
$$[\bar{Z}_{BB}]=[\bar{K}_{BB}-\omega^2\bar{M}_{BB}]$$
$$[\bar{Z}_{AA}]=[\bar{K}_{AA}-\omega^2\bar{M}_{AA}] \tag{10}$$

and the barred matrices are similar to the unbarred terms of Eq. (1), except that they pertain to the assembly of all components of the secondary structure, rather than just a single component, in contact with the primary structure. The derivation also shows that the rate of convergence depends on the magnitude of $|\lambda|_{\max}$. The convergence proof depends on a precise knowledge of the system frequency, thus, for static loadings ($\omega=0$), the proof is rigorous. However, for free-vibration problems, in which the frequency is approximated

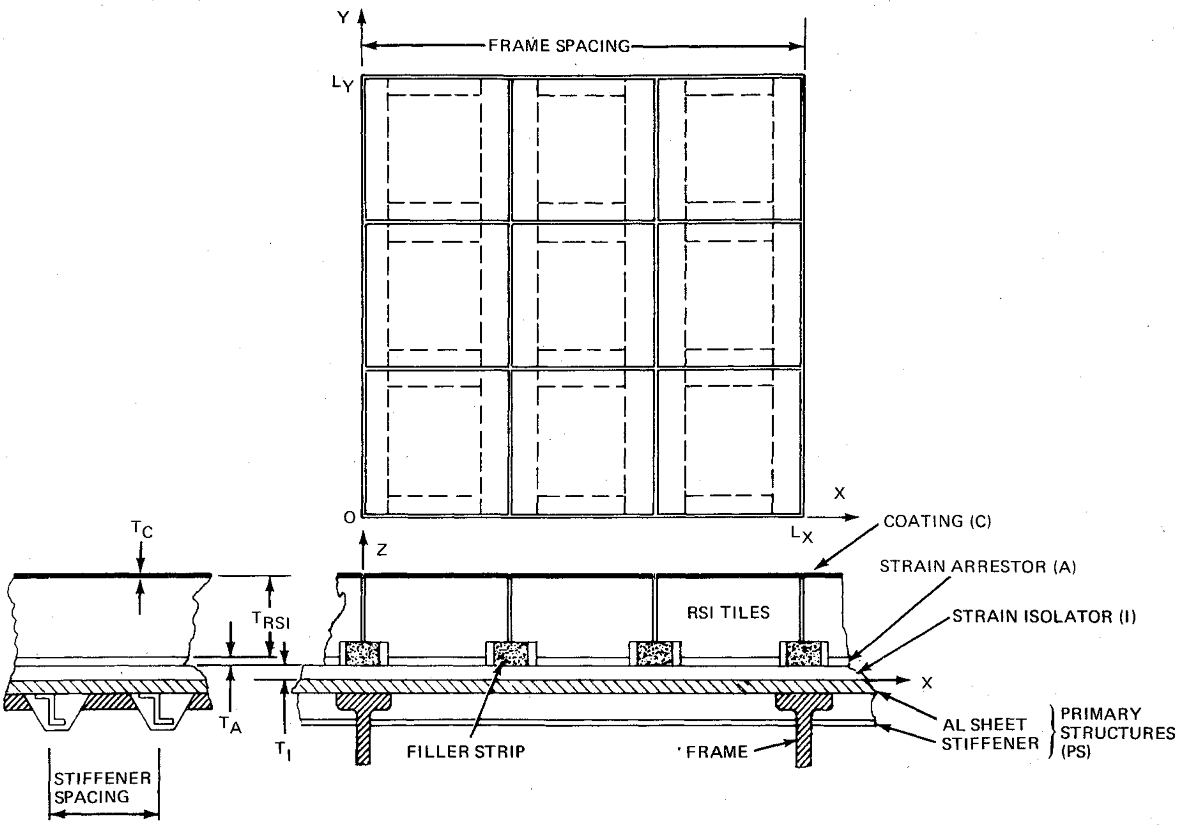

Fig. 5 Typical configuration for shuttle TPS.

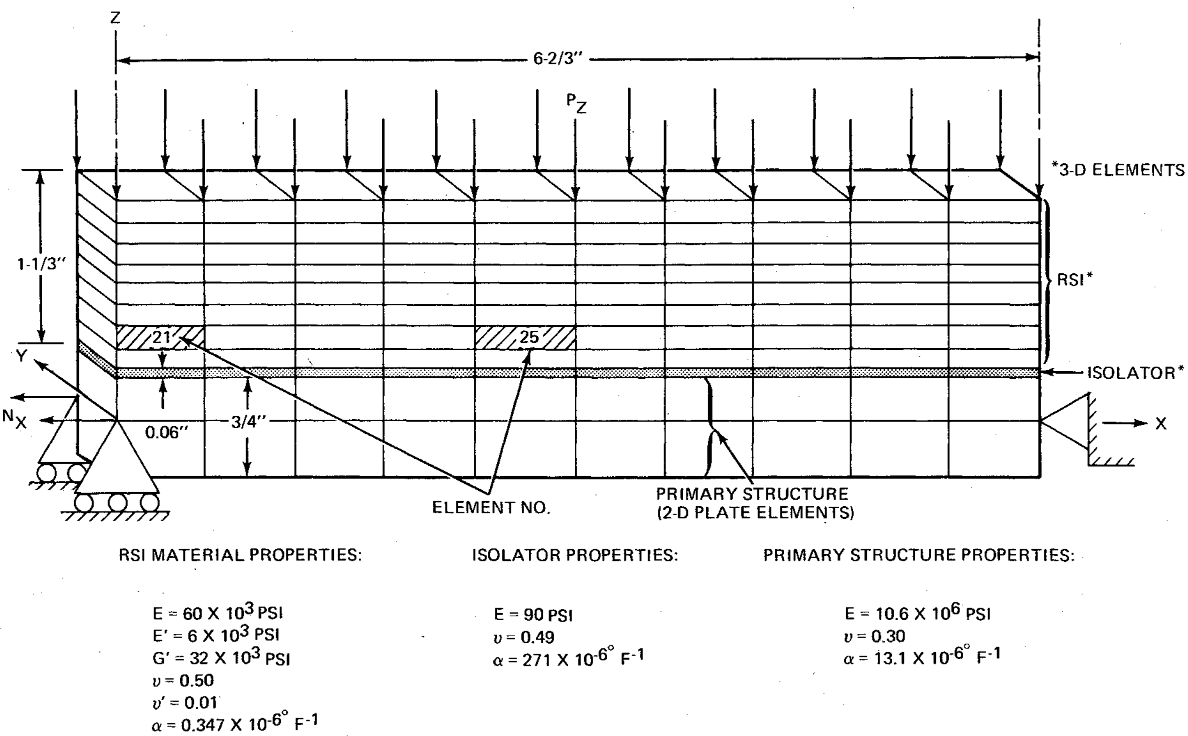

Fig. 6 Sample problem used to demonstrate numerical convergence of iteration scheme.

by a Rayleigh quotient based on the latest estimate of mode shapes, the proof is only heuristic.

A physical interpretation of the convergence condition stated in Eqs. (8) and (9) is that the impedance of the primary structure, $[Z_{ps}]$, must be "larger" than that of the components of the secondary structure, $[Z_S']$. Thus, even if the stiffness terms in $[Z_S']$ are small compared to $[Z_{ps}]$, when analyzing sufficiently high frequencies (ω), the presence of inertia terms could adversely affect convergence of the procedure.

Example – Space Shuttle Surface Insulation

The integrity of a reusable space shuttle system is strongly dependent on protecting the orbiting vehicle from re-entry heating in a manner which does not require significant refurbishment between missions. The thermal protection system

Table 1 Critical deflections and stresses vs iteration number (see Fig. 6)

Example 1: N_x = 40,125 lb/in., P_z = 0, ΔT = 0

Iteration No.	Avg σ_{xx}*, psi Elem No. 25	Avg σ_{xz}, psi Elem No. 21	Primary Structure u(x = 0) X 10^2 in.
1	17.33	3.497	-3.566
2	17.51	3.503	-3.565
3	17.51	3.503	-3.565
4	17.51	3.503	-3.565

Example 2: P_z = 100 psi, N_x = 0, ΔT = 0

Iteration No.	Avg σ_{xx}*, psi Elem No. 25	Avg σ_{xz}, psi Elem No. 21	Primary Structure w(x = 3-1/3 in.) X 10^3 in.
1	38.62	-3.145	-7.222
2	37.90	-3.068	-7.017
3	37.90	-3.068	-7.022
4	37.90	-3.068	-7.022

Example 3: ΔT = -325°F, N_x = 0, P_z = 0

Iteration No.	Avg σ_{xx}, psi Elem No. 25	Avg σ_{xz}, psi Elem No. 21	u(x = 0) X 10^2 in.
1	-16.38	-3.935	2.838
2	-16.75	-3.889	2.837
3	-16.74	-3.891	2.837
4	-16.74	-3.890	2.837

*Note that direct-stress allowables for RSI material in x and y directions are of the order of 30 psi.

Table 2 Fundamental frequency, maximum deflection, and critical tile stresses vs iteration number

			RSI Stresses					
			σ_x, psi Element No. 25			σ_z, psi Element No. 21		
Iteration No.	ω_1, Hz	Maximum Normalized Deflection, in.	Tile No. 1	Tile No. 2	Tile No. 3	Tile No. 1	Tile No. 2	Tile No. 3
0	510	0.180	-	-	-	-	-	-
1	425	0.181	-43	-88	-46	22	57	35
2	427	0.181	-40	-86	-43	22	49	28
3	425	0.181	-40	-86	-46	21	48	28
4	425	0.181	-40	-86	-46	22	49	28

Table 3 Fundamental frequency and maximum primary-structure deflection as a function of iteration number (see Fig. 7)

Iteration No.	Fundamental Frequency, Hz	Normalized Max Primary Structure Deflection, in.
0	146	0.111
1	153	0.108
2	153	0.111
3	154	0.110
4	153	0.110

(TPS) selected to fulfill this need is a nonstructural, reusable surface insulation (RSI) material shaped into individual tiles which cover almost all of the orbiter surface area. Most of the tiles are square in planform and measure 6×6 or 8×8 in., with thicknesses varying roughly between 0.5 and 3 in. Since loss of a single tile could be catastrophic, RSI tile stresses must be determined accurately for the anticipated static, dynamic, and thermal environments.

A detailed computer program, employing the current iterative procedure, was prepared to determine accurately the tile stresses associated with static loading, internal transient temperature states, and natural vibrations. Because of the complex geometry, nonuniform anisotropic material properties, and detailed three-dimensional stress states, the TPS was idealized by finite-element assemblages with up to 2,500 degrees of freedom per tile. Because of the large size of the problem and the diverse variation in the stiffness properties of the tiles and primary structure, solution of this problem through application of the standard direct-stiffness method, or even existing static and dynamic matrix coupling methods, was not practical. The present iteration scheme overcame these problems, by treating each tile separately. An important byproduct of this approach was that it avoided numerical conditioning problems associated with combining low-stiffness tile elements ($E \approx 50$ psi), used for isolation purposes, with high-stiffness primary-structure elements ($E \approx 10 \times 10^6$ psi).

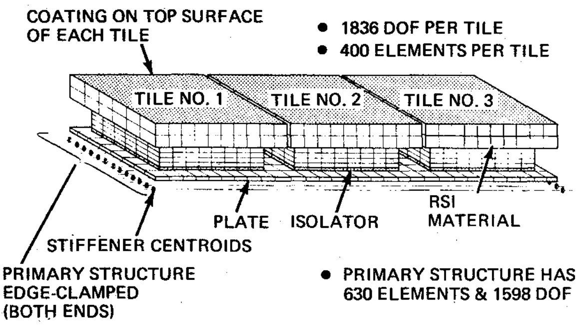

Fig. 7 Typical configuration that computer program is capable of analyzing.

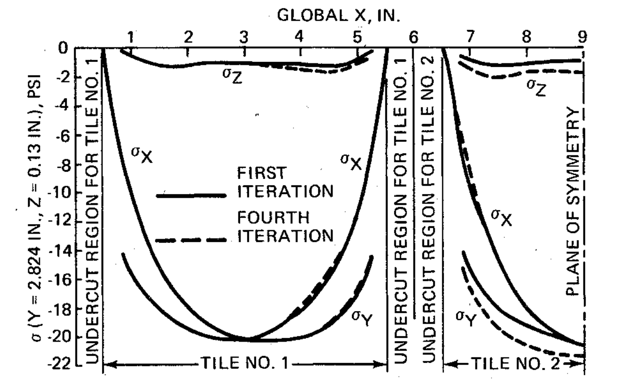

Fig. 8 Direct stresses for tiles 1 and 2 caused by -170°F cold soak.

Structural Configuration

The configuration for which the computer program was developed is shown in Fig. 5. It consists of a stringer-stiffened flat rectangular panel supporting a nonstructural TPS.

The TPS is composed of a series of rigidized RSI tiles. The tiles may or may not be undercut on all four sides to accommodate "filler strips." The purpose of the nonrigidized filler-strip insulation, if it is found necessary, will be to prevent severe heat penetration through the gaps between adjacent tiles.

The RSI material is not bonded directly to the primary structure, but to a thin, stiff "strain-isolator" material. The function of both these items is to help isolate the primary-structure strains from the low-strength RSI tiles, for the wide range of loading environments which the vehicle must sustain. If the strain-arrestor plate is unnecessary, a provision exists to remove it from the analysis. For details on the structural idealization and the computer program, refer to Refs. 2-4.

Numerical Results

Several RSI problems were run to demonstrate the numerical convergence properties of the iteration scheme. The material properties and loading conditions used, while not precise in a specific design sense, are representative of the problem parameters the method is intended to accommodate.

Figure 6 shows the configuration, finite-element idealization, and material properties for an example with

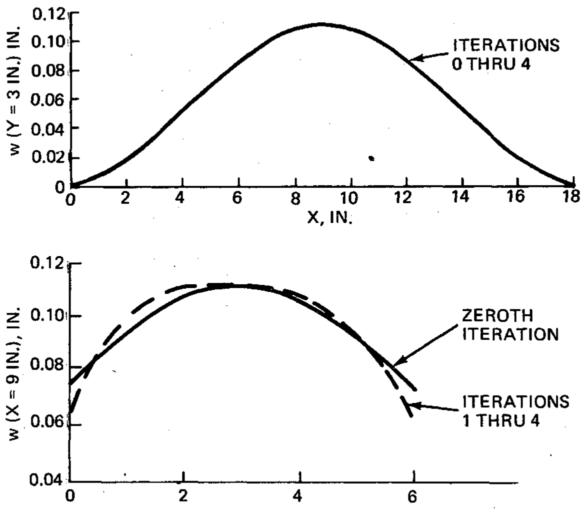

Fig. 9 Plate structure normal deflections of first mode.

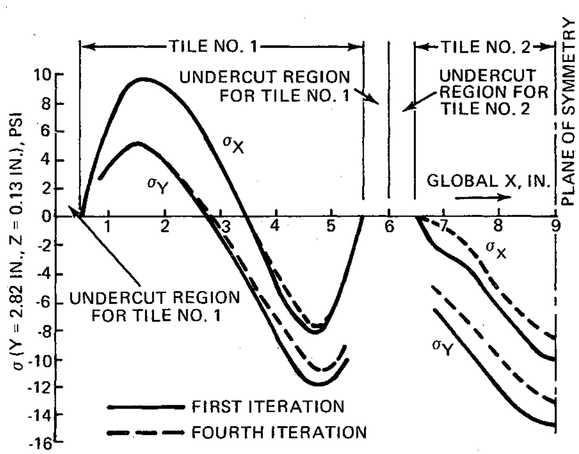

Fig. 10 Normalized first mode direct stresses for tiles 1 and 2 in planar directions as a function of spanwise coordinate.

three separate load cases. The largest primary-structure nodal deflections and average stress components for certain RSI elements are presented as a function of iteration number in Table 1. Although the stress levels appear quite low, note that the RSI material direct stress allowables are in the 30-psi range for the x, y directions and even lower from the z direction and shear allowables. Table 1 reveals a rapid convergence rate and a high level of accuracy for the initial approximation, in that the maximum error for the first iteration is less than 3% in all cases.

A problem similar to that depicted in Fig. 6 was run to illustrate the vibration capability; this time, a three-tile configuration with a 20-in. span was used. The fundamental frequency, largest primary-structure normalized deflection, and average stress components for certain critical RSI elements are presented as a function of iteration number in Table 2. Besides revealing a rapid convergence rate, the results presented indicate a high level of accuracy for the first iteration in that the maximum frequency, deflection, and σ_x errors are less than 2%. The errors in σ_z were higher for the first iteration (approximately 20%), but these settled down to under 4% in the second iteration.

These observations are further strengthened by the more realistic shuttle tile example shown in Fig. 7. This problem consists of a $-170°F$ cold soak of three 6×6-in. tiles, each of which are 2-in. thick and have 1×1/2-in. edge undercuts. The primary structure is a 0.041-in. aluminum plate with offset stringers spaced 1/2 in. apart. Two opposite boundaries were held against out-of-plane deflection with the other two ends free. To permit free thermal contractions, in-plane plate motion was permitted.

The resulting direct stresses for the first and fourth iterations are plotted in Fig. 8 for tiles 1 and 2. Because the differences were so slight, only second and fourth iteration values for σ_x are plotted. The fundamental frequency and peak normalized deflection, as a function of iteration number, were also obtained for this configuration, and are shown in Table 3. The primary-structure mode shape is plotted in Fig. 9 for iterations 0 through 4. Some typical corresponding stress components for iterations 1 and 4 are shown in Fig. 10.

Conclusions

An efficient iterative procedure has been presented for the static mechanical, thermal stress, and vibration analysis of component structures with widely differing stiffnesses. The vibration results can easily be extended to solve dynamics problems through modal superposition procedures. The method, which is quite general, converges under the conditions defined in Eqs. (6-8). Because of the complexity of the structure and the rapid rate of convergence, the procedure is ideally suited for further RSI shuttle-panel studies.

References

[1]Newman, M. and Goldberg, M., private communication, Polytechnic Institute of New York, 1963.

[2]Ojalvo, I.U., Levy, A., and Austin, F., "Thermal Stress Analysis of Reusable Surface Insulation for Shuttle," NASA CR-132502, Sept. 1974.

[3]Ojalvo, I.U., Austin, F., and Levy, A., "Vibration and Stress Analysis of Soft-Bonded Shuttle Insulation Tiles," NASA CR-132553, Sept. 1974.

[4]Ojalvo, I.U., Levy, A., and Austin, F., "A Method for the Dynamic and Thermal Stress Analysis of Space Shuttle Surface Insulation," AIAA Paper 75-801, Denver, Colo., May 1975.

[5]Austin, F. and Ojalvo, I.U., "Convergence of an Iterative Procedure for Large-Scale Static Analysis of Structural Components," *AIAA Journal*, Vol. 14, No. 1, 1976, pp. 104-106.